High order positivity-preserving entropy stable discontinuous Galerkin discretizations

Jesse Chan

Dept. of Computational Applied Mathematics and Operations Research
Rice University

FEM@LLNL: MFEM Seminar, Lawrence Livermore National Laboratories

Former PhD student: Dr. Yimin Lin

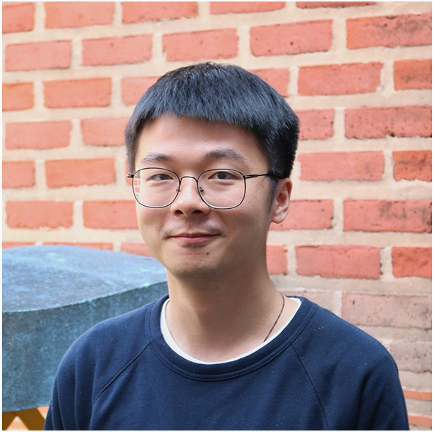

Yimin has been the driving force behind the work in this talk.

High order finite element methods for hyperbolic PDEs

- Fluid dynamics applications: acoustics, vorticular flows, turbulence, shocks.
- Goal: high accuracy on unstructured meshes.
- Discontinuous Galerkin (DG) methods: geometric flexibility + high order.

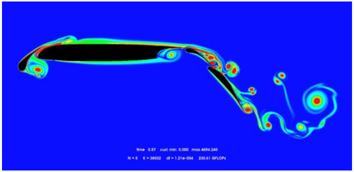

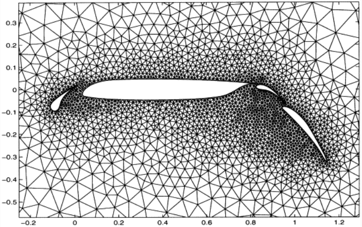

Mesh from Slawig 2001.

High order finite element methods for hyperbolic PDEs

- Fluid dynamics applications: acoustics, vorticular flows, turbulence, shocks.
- Goal: high accuracy on unstructured meshes.
- Discontinuous Galerkin (DG) methods: geometric flexibility + high order.

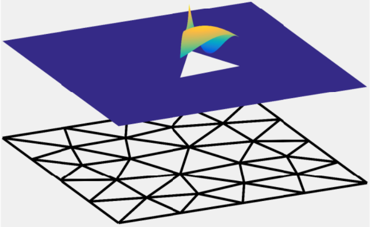

Why discontinuous Galerkin methods?

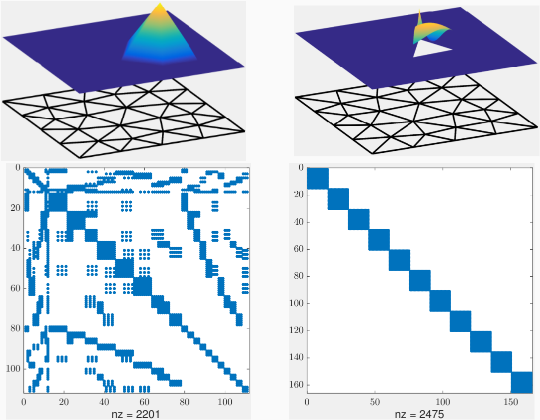

(a) High order FEM **(b)** High order DG

High order DG mass matrices: easily invertible for explicit time-stepping.

Why high order accuracy?

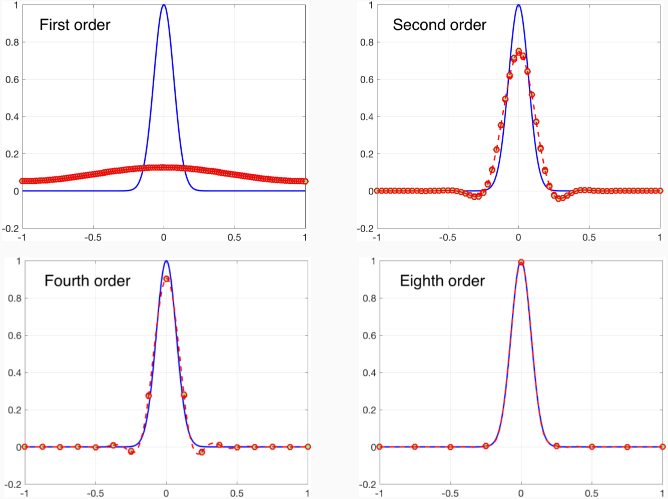

Accurate resolution of propagating vortices and waves.

Why high order accuracy?

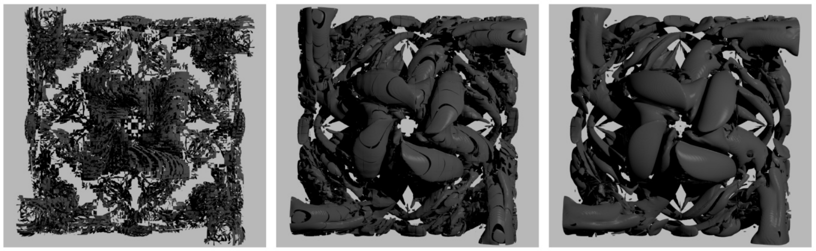

2nd, 4th, and 16th order Taylor-Green vortex. Vorticular structures and acoustic waves are both sensitive to numerical dissipation.

Results from Beck and Gassner (2013).

Why *not* high order DG methods?

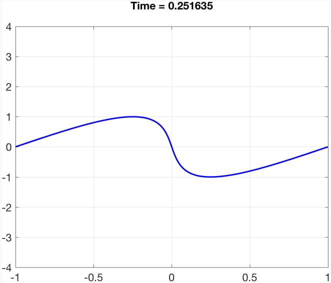

(a) Exact solution

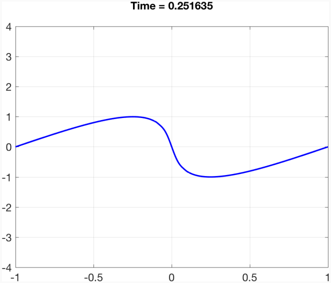

(b) 8th order DG

High order methods blow up for under-resolved solutions of nonlinear conservation laws (e.g., shocks and turbulence).

Why *not* high order DG methods?

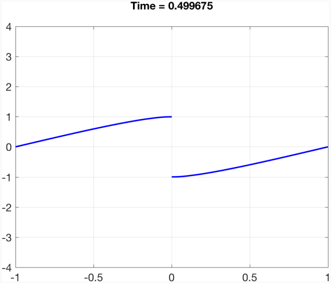

(a) Exact solution

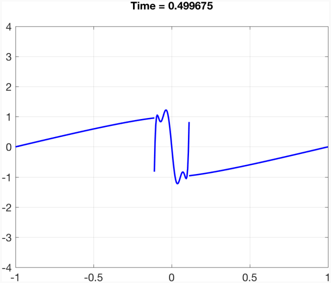

(b) 8th order DG

High order methods blow up for under-resolved solutions of nonlinear conservation laws (e.g., shocks and turbulence).

Why *not* high order DG methods?

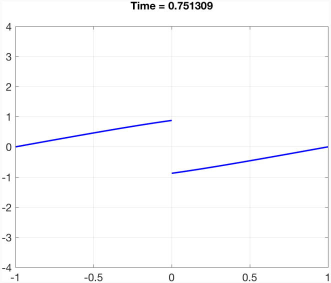

(a) Exact solution

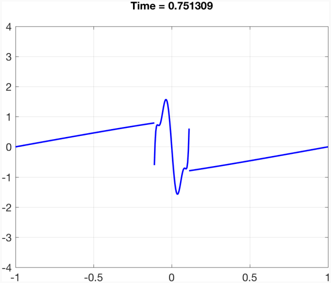

(b) 8th order DG

High order methods blow up for under-resolved solutions of nonlinear conservation laws (e.g., shocks and turbulence).

Why *not* high order DG methods?

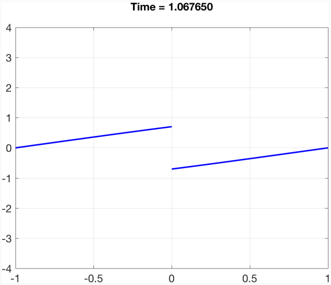

(a) Exact solution

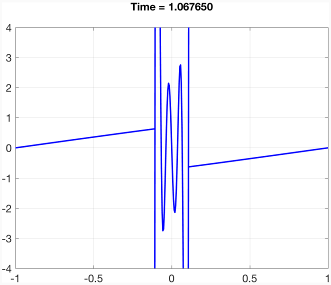

(b) 8th order DG

High order methods blow up for under-resolved solutions of nonlinear conservation laws (e.g., shocks and turbulence).

Why entropy stability for high order schemes?

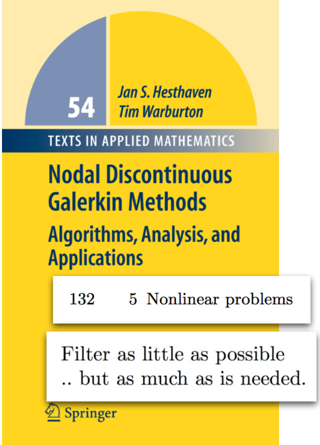

- High order DG needs heuristic stabilization (e.g., artificial viscosity, filtering).
- Entropy stable schemes improve robustness without *no added dissipation*.
- Turns DG into a “good” high order method.

Finite volume methods: Tadmor, Chandrashekar, Ray, Svard, Fjordholm, Mishra, LeFloch, Rohde, . . .
High order DGSEM: Fisher, Carpenter, Gassner, Winters, Kopriva, Persson, Pazner, . . .
High order simplices: Chen and Shu, Crean, Hicken, Del Rey Fernandez, Zingg, . . .

Examples of high order entropy stable DG simulations

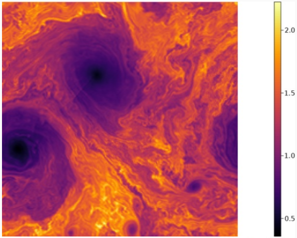

(a) Density, ρ.

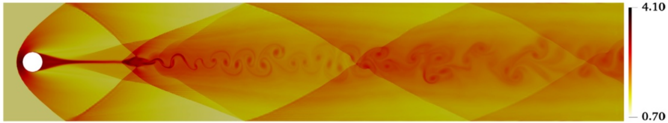

(b) Temperature, $\mathcal{T}$.

All simulations are run without artificial viscosity, filtering, or slope limiting.

Parsani et al. (2021). *High-order accurate entropy-stable discontinuous collocated Galerkin …*

Talk outline

1. Entropy stable nodal DG methods
2. Entropy stable nodal DG with positivity-preserving limiting
3. From subcell limiting to a cell entropy inequality

Entropy stable nodal DG methods

Entropy stability for nonlinear problems

- Energy balance for nonlinear conservation laws (Burgers', shallow water, compressible Euler + Navier-Stokes).

$$\frac{\partial \boldsymbol{u}}{\partial t} + \frac{\partial \boldsymbol{f}(\boldsymbol{u})}{\partial x} = 0.$$

- Continuous entropy inequality: convex entropy function $S(\boldsymbol{u})$, entropy potential $\psi(\boldsymbol{u})$, entropy variables $\boldsymbol{v}(\boldsymbol{u})$

$$\int_\Omega \boldsymbol{v}^T \left(\frac{\partial \boldsymbol{u}}{\partial t} + \frac{\partial \boldsymbol{f}(\boldsymbol{u})}{\partial x} \right) = 0, \qquad \boxed{\boldsymbol{v}(\boldsymbol{u}) = \frac{\partial S}{\partial \boldsymbol{u}}}$$

$$\implies \int_\Omega \frac{\partial S(\boldsymbol{u})}{\partial t} + \left(\boldsymbol{v}^T \boldsymbol{f}(\boldsymbol{u}) - \psi(\boldsymbol{u}) \right) \Big|_{-1}^{1} \leq 0.$$

Entropy conservative finite volume methods

- Finite volume scheme:

$$\frac{\mathrm{d}\mathbf{u}_i}{\mathrm{dt}} + \frac{\boldsymbol{f}(\mathbf{u}_{i+1}, \mathbf{u}_i) - \boldsymbol{f}(\mathbf{u}_i, \mathbf{u}_{i-1})}{h} = \mathbf{0}.$$

- Take $\boldsymbol{f} = \boldsymbol{f}_{EC}$ to be an entropy conservative numerical flux

$$\begin{aligned} \boldsymbol{f}_{EC}(\boldsymbol{u}, \boldsymbol{u}) &= \boldsymbol{f}(\boldsymbol{u}), && \text{(consistency)} \\ \boldsymbol{f}_{EC}(\boldsymbol{u}, \boldsymbol{v}) &= \boldsymbol{f}_{EC}(\boldsymbol{v}, \boldsymbol{u}), && \text{(symmetry)} \\ (\boldsymbol{v}_L - \boldsymbol{v}_R)^T \boldsymbol{f}_{EC}(\boldsymbol{u}_L, \boldsymbol{u}_R) &= \psi_L - \psi_R, && \text{(conservation).} \end{aligned}$$

- Can show numerical scheme conserves entropy

$$\int_\Omega \frac{\partial S(\boldsymbol{u})}{\partial t} \approx \sum_i h \frac{\mathrm{d}S(\mathbf{u}_i)}{\mathrm{dt}} = 0.$$

Tadmor (1987). *The numerical viscosity of entropy stable schemes for systems of conservation laws.*

Example of EC fluxes (compressible Euler equations)

- Define average $\{\{u\}\} = \frac{1}{2}(u_L + u_R)$. In one dimension:

$$
\begin{aligned}
f_S^1(\boldsymbol{u}_L, \boldsymbol{u}_R) &= \{\{\rho\}\}^{\log} \{\{u\}\} \\
f_S^2(\boldsymbol{u}_L, \boldsymbol{u}_R) &= \{\{u\}\} f_S^1 + p_{\text{avg}} \\
f_S^3(\boldsymbol{u}_L, \boldsymbol{u}_R) &= (E_{\text{avg}} + p_{\text{avg}}) \{\{u\}\},
\end{aligned}
$$

$$
p_{\text{avg}} = \frac{\{\{\rho\}\}}{2\{\{\beta\}\}}, \qquad E_{\text{avg}} = \frac{\{\{\rho\}\}^{\log}}{2\{\{\beta\}\}^{\log}(\gamma - 1)} + \frac{1}{2} u_L u_R.
$$

- Non-standard logarithmic mean, "inverse temperature" β

$$
\{\{u\}\}^{\log} = \frac{u_L - u_R}{\log u_L - \log u_R}, \qquad \beta = \frac{\rho}{2p}.
$$

Chandreshekar (2013), *Kinetic energy preserving and entropy stable finite volume schemes for the compressible Euler and Navier-Stokes equations.*

Matrix reformulation using Hadamard products

Hadamard product of two matrices $\mathbf{A} \circ \mathbf{B}$

$$\begin{bmatrix} \mathbf{A}_{11} & \dots & \mathbf{A}_{1n} \\ \vdots & \ddots & \vdots \\ \mathbf{A}_{n1} & \dots & \mathbf{A}_{nn} \end{bmatrix} \circ \begin{bmatrix} \mathbf{B}_{11} & \dots & \mathbf{B}_{1n} \\ \vdots & \ddots & \vdots \\ \mathbf{B}_{n1} & \dots & \mathbf{B}_{nn} \end{bmatrix} = \begin{bmatrix} \mathbf{A}_{11}\mathbf{B}_{11} & \dots & \mathbf{A}_{1n}\mathbf{B}_{1n} \\ \vdots & \ddots & \vdots \\ \mathbf{A}_{n1}\mathbf{B}_{n1} & \dots & \mathbf{A}_{nn}\mathbf{B}_{nn} \end{bmatrix}.$$

Rewrite an N-point (periodic) finite volume scheme as

$$\frac{\mathrm{d}}{\mathrm{dt}} \begin{bmatrix} \mathbf{u}_1 \\ \mathbf{u}_2 \\ \vdots \\ \mathbf{u}_N \end{bmatrix} + \frac{1}{h} \begin{bmatrix} f_{EC}(\mathbf{u}_1, \mathbf{u}_2) - f_{EC}(\mathbf{u}_N, \mathbf{u}_1) \\ f_{EC}(\mathbf{u}_2, \mathbf{u}_3) - f_{EC}(\mathbf{u}_1, \mathbf{u}_2) \\ \vdots \\ f_{EC}(\mathbf{u}_N, \mathbf{u}_1) - f_{EC}(\mathbf{u}_{N-1}, \mathbf{u}_N) \end{bmatrix} = \mathbf{0}.$$

Matrix reformulation using Hadamard products

Hadamard product of two matrices $\mathbf{A} \circ \mathbf{B}$

$$\begin{bmatrix} \mathbf{A}_{11} & \dots & \mathbf{A}_{1n} \\ \vdots & \ddots & \vdots \\ \mathbf{A}_{n1} & \dots & \mathbf{A}_{nn} \end{bmatrix} \circ \begin{bmatrix} \mathbf{B}_{11} & \dots & \mathbf{B}_{1n} \\ \vdots & \ddots & \vdots \\ \mathbf{B}_{n1} & \dots & \mathbf{B}_{nn} \end{bmatrix} = \begin{bmatrix} \mathbf{A}_{11}\mathbf{B}_{11} & \dots & \mathbf{A}_{1n}\mathbf{B}_{1n} \\ \vdots & \ddots & \vdots \\ \mathbf{A}_{n1}\mathbf{B}_{n1} & \dots & \mathbf{A}_{nn}\mathbf{B}_{nn} \end{bmatrix}.$$

Rewrite an N-point (periodic) finite volume scheme as

$$\frac{\mathrm{d}}{\mathrm{dt}} \begin{bmatrix} \mathbf{u}_1 \\ \mathbf{u}_2 \\ \vdots \\ \mathbf{u}_N \end{bmatrix} + \frac{1}{h} \begin{bmatrix} \boldsymbol{f}_{EC}(\mathbf{u}_1, \mathbf{u}_2) - \boldsymbol{f}_{EC}(\mathbf{u}_N, \mathbf{u}_1) \\ \boldsymbol{f}_{EC}(\mathbf{u}_2, \mathbf{u}_3) - \boldsymbol{f}_{EC}(\mathbf{u}_1, \mathbf{u}_2) \\ \vdots \\ \boldsymbol{f}_{EC}(\mathbf{u}_N, \mathbf{u}_1) - \boldsymbol{f}_{EC}(\mathbf{u}_{N-1}, \mathbf{u}_N) \end{bmatrix} = \mathbf{0}.$$

Matrix reformulation using Hadamard products

Hadamard product of two matrices $\mathbf{A} \circ \mathbf{B}$

$$\begin{bmatrix} \mathbf{A}_{11} & \dots & \mathbf{A}_{1n} \\ \vdots & \ddots & \vdots \\ \mathbf{A}_{n1} & \dots & \mathbf{A}_{nn} \end{bmatrix} \circ \begin{bmatrix} \mathbf{B}_{11} & \dots & \mathbf{B}_{1n} \\ \vdots & \ddots & \vdots \\ \mathbf{B}_{n1} & \dots & \mathbf{B}_{nn} \end{bmatrix} = \begin{bmatrix} \mathbf{A}_{11}\mathbf{B}_{11} & \dots & \mathbf{A}_{1n}\mathbf{B}_{1n} \\ \vdots & \ddots & \vdots \\ \mathbf{A}_{n1}\mathbf{B}_{n1} & \dots & \mathbf{A}_{nn}\mathbf{B}_{nn} \end{bmatrix}.$$

Rewrite an N-point (periodic) finite volume scheme as

$$h\frac{\mathrm{d}}{\mathrm{dt}}\begin{bmatrix} \mathbf{u}_1 \\ \mathbf{u}_2 \\ \vdots \\ \mathbf{u}_N \end{bmatrix} + \begin{bmatrix} \mathbf{F}_{1,2} - \mathbf{F}_{1,N} \\ \mathbf{F}_{2,3} - \mathbf{F}_{2,1} \\ \vdots \\ \mathbf{F}_{N,1} - \mathbf{F}_{N,N-1} \end{bmatrix} = \mathbf{0}, \qquad \mathbf{F}_{ij} = \boldsymbol{f}_{EC}(\mathbf{u}_i, \mathbf{u}_j).$$

Matrix reformulation using Hadamard products

Hadamard product of two matrices $\mathbf{A} \circ \mathbf{B}$

$$\begin{bmatrix} \mathbf{A}_{11} & \dots & \mathbf{A}_{1n} \\ \vdots & \ddots & \vdots \\ \mathbf{A}_{n1} & \dots & \mathbf{A}_{nn} \end{bmatrix} \circ \begin{bmatrix} \mathbf{B}_{11} & \dots & \mathbf{B}_{1n} \\ \vdots & \ddots & \vdots \\ \mathbf{B}_{n1} & \dots & \mathbf{B}_{nn} \end{bmatrix} = \begin{bmatrix} \mathbf{A}_{11}\mathbf{B}_{11} & \dots & \mathbf{A}_{1n}\mathbf{B}_{1n} \\ \vdots & \ddots & \vdots \\ \mathbf{A}_{n1}\mathbf{B}_{n1} & \dots & \mathbf{A}_{nn}\mathbf{B}_{nn} \end{bmatrix}.$$

Rewrite an N-point (periodic) finite volume scheme as

$$\begin{bmatrix} \mathbf{F}_{1,2} - \mathbf{F}_{1,N} \\ \mathbf{F}_{2,3} - \mathbf{F}_{2,1} \\ \vdots \\ \mathbf{F}_{N,1} - \mathbf{F}_{N,N-1} \end{bmatrix} = \left(\begin{bmatrix} 0 & 1 & & -1 \\ -1 & 0 & 1 & \\ & \ddots & \ddots & 1 \\ 1 & & -1 & 0 \end{bmatrix} \circ \begin{bmatrix} \mathbf{F}_{1,1} & \dots & \mathbf{F}_{1,N} \\ \vdots & \ddots & \vdots \\ \mathbf{F}_{N,1} & \dots & \mathbf{F}_{N,N} \end{bmatrix} \right) \mathbf{1}.$$

Matrix reformulation using Hadamard products

Hadamard product of two matrices $\mathbf{A} \circ \mathbf{B}$

$$\begin{bmatrix} \mathbf{A}_{11} & \dots & \mathbf{A}_{1n} \\ \vdots & \ddots & \vdots \\ \mathbf{A}_{n1} & \dots & \mathbf{A}_{nn} \end{bmatrix} \circ \begin{bmatrix} \mathbf{B}_{11} & \dots & \mathbf{B}_{1n} \\ \vdots & \ddots & \vdots \\ \mathbf{B}_{n1} & \dots & \mathbf{B}_{nn} \end{bmatrix} = \begin{bmatrix} \mathbf{A}_{11}\mathbf{B}_{11} & \dots & \mathbf{A}_{1n}\mathbf{B}_{1n} \\ \vdots & \ddots & \vdots \\ \mathbf{A}_{n1}\mathbf{B}_{n1} & \dots & \mathbf{A}_{nn}\mathbf{B}_{nn} \end{bmatrix}.$$

Rewrite an N-point (periodic) finite volume scheme as

$$\begin{bmatrix} \mathbf{F}_{1,2} - \mathbf{F}_{1,N} \\ \mathbf{F}_{2,3} - \mathbf{F}_{2,1} \\ \vdots \\ \mathbf{F}_{N,1} - \mathbf{F}_{N,N-1} \end{bmatrix} = \Bigg(\underbrace{\begin{bmatrix} 0 & 1 & & -1 \\ -1 & 0 & 1 & \\ & \ddots & \ddots & 1 \\ 1 & & -1 & 0 \end{bmatrix}}_{\text{periodic central difference}} \circ \underbrace{\begin{bmatrix} \mathbf{F}_{1,1} & \dots & \mathbf{F}_{1,N} \\ \vdots & \ddots & \vdots \\ \mathbf{F}_{N,1} & \dots & \mathbf{F}_{N,N} \end{bmatrix}}_{\text{flux matrix } \mathbf{F}} \Bigg) \mathbf{1}.$$

Matrix reformulation using Hadamard products

Hadamard product of two matrices $\mathbf{A} \circ \mathbf{B}$

$$\begin{bmatrix} \mathbf{A}_{11} & \dots & \mathbf{A}_{1n} \\ \vdots & \ddots & \vdots \\ \mathbf{A}_{n1} & \dots & \mathbf{A}_{nn} \end{bmatrix} \circ \begin{bmatrix} \mathbf{B}_{11} & \dots & \mathbf{B}_{1n} \\ \vdots & \ddots & \vdots \\ \mathbf{B}_{n1} & \dots & \mathbf{B}_{nn} \end{bmatrix} = \begin{bmatrix} \mathbf{A}_{11}\mathbf{B}_{11} & \dots & \mathbf{A}_{1n}\mathbf{B}_{1n} \\ \vdots & \ddots & \vdots \\ \mathbf{A}_{n1}\mathbf{B}_{n1} & \dots & \mathbf{A}_{nn}\mathbf{B}_{nn} \end{bmatrix}.$$

Rewrite an N-point (periodic) finite volume scheme as

$$\begin{bmatrix} \mathbf{F}_{1,2} - \mathbf{F}_{1,N} \\ \mathbf{F}_{2,3} - \mathbf{F}_{2,1} \\ \vdots \\ \mathbf{F}_{N,1} - \mathbf{F}_{N,N-1} \end{bmatrix} = 2(\mathbf{Q} \circ \mathbf{F})\mathbf{1}.$$

Interpretation using finite difference matrices

Let $\mathbf{M} = h\mathbf{I}$. Can reformulate entropy conservative finite volume as

$$\mathbf{M}\frac{\mathrm{d}\mathbf{u}}{\mathrm{dt}} + 2\left(\mathbf{Q} \circ \mathbf{F}\right)\mathbf{1} = \mathbf{0}, \qquad \mathbf{Q} = \frac{1}{2}\begin{bmatrix} 0 & 1 & & -1 \\ -1 & 0 & 1 & \\ & \ddots & \ddots & 1 \\ 1 & & -1 & 0 \end{bmatrix}$$

Note: $\mathbf{M}^{-1}\mathbf{Q}$ is a 2nd order (periodic) differentiation matrix.

Key result: generalizable beyond finite volumes

Entropy conservation for any $\underbrace{\mathbf{Q} = -\mathbf{Q}^T}_{\text{skew-symmetry}}$ and $\underbrace{\mathbf{Q1} = \mathbf{0}}_{\text{conservative}}$!

Interpretation using finite difference matrices

Let $\mathbf{M} = h\mathbf{I}$. Can reformulate entropy conservative finite volume as

$$\mathbf{M}\frac{\mathrm{d}\mathbf{u}}{\mathrm{dt}} + 2\left(\mathbf{Q} \circ \mathbf{F}\right)\mathbf{1} = \mathbf{0}, \qquad \mathbf{Q} = \frac{1}{2}\begin{bmatrix} 0 & 1 & & -1 \\ -1 & 0 & 1 & \\ & \ddots & \ddots & 1 \\ 1 & & -1 & 0 \end{bmatrix}$$

Note: $\mathbf{M}^{-1}\mathbf{Q}$ is a 2nd order (periodic) differentiation matrix.

Key result: generalizable beyond finite volumes

Entropy conservation for any $\underbrace{\mathbf{Q} = -\mathbf{Q}^T}_{\text{skew-symmetry}}$ and $\underbrace{\mathbf{Q}\mathbf{1} = \mathbf{0}}_{\text{conservative}}$!

A brief intro to nodal discontinuous Galerkin methods

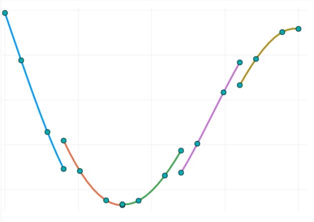

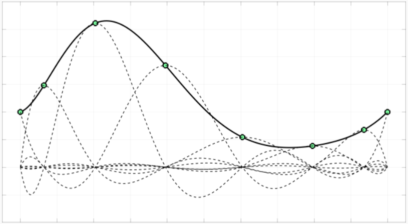

- Multiply by nodal (Lagrange) basis $\ell_i(x)$ and integrate

$$\int_{D^k} \left(\frac{\partial \boldsymbol{u}}{\partial t} + \frac{\partial \boldsymbol{f}(\boldsymbol{u})}{\partial x} \right) \ell_i + \int_{\partial D^k} (\boldsymbol{f}^*(\boldsymbol{u}^+, \boldsymbol{u}^-) - \boldsymbol{f}(\boldsymbol{u}^-)) n \ell_i = 0$$

- The numerical flux $\boldsymbol{f}^*(\boldsymbol{u}^+, \boldsymbol{u}^-) \approx \boldsymbol{f}(\boldsymbol{u})$ enforces boundary conditions and weak continuity across interfaces.
- Nodal (collocation) DG methods: use Gauss-Lobatto quadrature nodes for both interpolation and integration.

Matrix formulation of nodal DG methods

- Map integrals to the reference interval $\widehat{D} = [-1, 1]$

$$\int_{\widehat{D}} \left(\frac{h}{2} \frac{\partial \boldsymbol{u}}{\partial t} + \frac{\partial \boldsymbol{f}(\boldsymbol{u})}{\partial x} \right) \ell_i + \int_{\partial \widehat{D}} (\boldsymbol{f}^*(\boldsymbol{u}^+, \boldsymbol{u}^-) - \boldsymbol{f}(\boldsymbol{u}^-)) n \ell_i = 0$$

- Use $\boldsymbol{u}(x,t) = \sum_j \boldsymbol{u}_j(t) \ell_j(x)$ and $\int_{-1}^{1} \frac{\partial \boldsymbol{f}(\boldsymbol{u})}{\partial x} \ell_i \approx \mathbf{Q} \boldsymbol{f}(\mathbf{u})$

$$\mathbf{M} \frac{\mathrm{d}\mathbf{u}}{\mathrm{dt}} + \mathbf{Q} \boldsymbol{f}(\mathbf{u}) + \mathbf{E}^T \mathbf{B} \Big(\underbrace{\boldsymbol{f}^* \left(\mathbf{u}^+, \mathbf{u}^- \right)}_{\text{interface flux}} - \boldsymbol{f}(\mathbf{u}^-) \Big) = \mathbf{0}.$$

where $\mathbf{M} = \frac{h}{2} \operatorname{diag}(w_1, \ldots, w_{N+1})$, and $\mathbf{Q}, \mathbf{B}, \mathbf{E}$ are differentiation and boundary matrices

$$\mathbf{Q}_{ij} = \int_{-1}^{1} \frac{\partial \ell_j}{\partial x} \ell_i, \quad \mathbf{B} = \begin{bmatrix} -1 & 0 \\ 0 & 1 \end{bmatrix}, \quad \mathbf{E} = \begin{bmatrix} 1 & 0 & \ldots & 0 \\ 0 & \ldots & 0 & 1 \end{bmatrix}.$$

A "flux differencing" formulation

- Idea: reformulate the DG flux derivative term

$$\int_{-1}^{1} \frac{\partial \boldsymbol{f}(\boldsymbol{u})}{\partial x} \ell_i \approx \mathbf{Q} \boldsymbol{f}(\mathbf{u}).$$

- Note that $\mathbf{Q1} = \mathbf{0}$, so $\sum_j \mathbf{Q}_{ij} = 0$. Thus,

$$(\mathbf{Q}\boldsymbol{f}(\mathbf{u}))_i = \sum_j \mathbf{Q}_{ij} \left(\boldsymbol{f}(\mathbf{u}_j) + \boldsymbol{f}(\mathbf{u}_i)\right) = 2\sum_j \mathbf{Q}_{ij} \underbrace{\frac{\boldsymbol{f}(\mathbf{u}_j) + \boldsymbol{f}(\mathbf{u}_i)}{2}}_{\text{central flux}}$$

- We replace the central flux with an entropy conservative flux

$$2\sum_j \mathbf{Q}_{ij} \boldsymbol{f}_{EC}(\mathbf{u}_i, \mathbf{u}_j) = \left(2\left(\mathbf{Q} \circ \mathbf{F}\right)\mathbf{1}\right)_i, \quad \mathbf{F}_{ij} = \boldsymbol{f}_{EC}(\mathbf{u}_i, \mathbf{u}_j).$$

Extension to multiple elements

- An entropy stable nodal DG formulation can be written as:

$$\mathbf{M}\frac{\mathrm{d}\mathbf{u}}{\mathrm{dt}} + \mathbf{Q}\boldsymbol{f}(\mathbf{u}) + \mathbf{E}^T\mathbf{B}\Big(\underbrace{\boldsymbol{f}^*\left(\mathbf{u}^+, \mathbf{u}^-\right)}_{\text{interface flux}} - \boldsymbol{f}(\mathbf{u}^-)\Big) = \mathbf{0}.$$

- If $\mathbf{Q}$ satisfies the summation-by-parts (SBP) property

$$\mathbf{Q} + \mathbf{Q}^T = \mathbf{E}^T\mathbf{B}\mathbf{E}$$

and if $\boldsymbol{f}^*\left(\mathbf{u}^+, \mathbf{u}\right)$ is entropy stable (e.g., local Lax-Friedrichs flux), a cell entropy inequality holds:

$$\boxed{\int_{D^k} \frac{\partial S(\boldsymbol{u})}{\partial t} + \int_{\partial D^k} \left(\boldsymbol{v}^T\boldsymbol{f}^*(\boldsymbol{u}^+, \boldsymbol{u}^-) - \psi\left(\boldsymbol{u}\right)\right) n \leq 0.}$$

Fisher and Carpenter (2014), Gassner, Winters, and Kopriva (2016), Chen and Shu (2017), etc.

- An entropy stable nodal DG formulation can be written as:

$$\mathbf{M}\frac{\mathrm{d}\mathbf{u}}{\mathrm{dt}} + 2\left(\mathbf{Q}\circ\mathbf{F}\right)\mathbf{1} + \mathbf{E}^T\mathbf{B}\Big(\underbrace{\boldsymbol{f}^*\left(\mathbf{u}^+,\mathbf{u}^-\right)}_{\text{interface flux}} - \boldsymbol{f}(\mathbf{u}^-)\Big) = \mathbf{0}.$$

- If $\mathbf{Q}$ satisfies the summation-by-parts (SBP) property

$$\mathbf{Q} + \mathbf{Q}^T = \mathbf{E}^T\mathbf{B}\mathbf{E}$$

and if $\boldsymbol{f}^*\left(\mathbf{u}^+,\mathbf{u}\right)$ is entropy stable (e.g., local Lax-Friedrichs flux), a cell entropy inequality holds:

$$\boxed{\int_{D^k}\frac{\partial S(\boldsymbol{u})}{\partial t} + \int_{\partial D^k}\left(\boldsymbol{v}^T\boldsymbol{f}^*(\boldsymbol{u}^+,\boldsymbol{u}^-) - \psi\left(\boldsymbol{u}\right)\right)n \leq 0.}$$

Fisher and Carpenter (2014), Gassner, Winters, and Kopriva (2016), Chen and Shu (2017), etc.

Extension to multiple elements

- An entropy stable nodal DG formulation can be written as:

$$\mathbf{M}\frac{\mathrm{d}\mathbf{u}}{\mathrm{d}t} + 2\left(\mathbf{Q}\circ\mathbf{F}\right)\mathbf{1} + \mathbf{E}^T\mathbf{B}\Big(\underbrace{\boldsymbol{f}^*\left(\mathbf{u}^+,\mathbf{u}^-\right)}_{\text{interface flux}} - \boldsymbol{f}(\mathbf{u}^-)\Big) = \mathbf{0}.$$

- If $\mathbf{Q}$ satisfies the summation-by-parts (SBP) property

$$\mathbf{Q} + \mathbf{Q}^T = \mathbf{E}^T\mathbf{B}\mathbf{E}$$

and if $\boldsymbol{f}^*\left(\mathbf{u}^+,\mathbf{u}\right)$ is entropy stable (e.g., local Lax-Friedrichs flux), a cell entropy inequality holds:

$$\boxed{\int_{D^k}\frac{\partial S(\boldsymbol{u})}{\partial t} + \int_{\partial D^k}\left(\boldsymbol{v}^T\boldsymbol{f}^*(\boldsymbol{u}^+,\boldsymbol{u}^-) - \psi\left(\boldsymbol{u}\right)\right)n \leq 0.}$$

Fisher and Carpenter (2014), Gassner, Winters, and Kopriva (2016), Chen and Shu (2017), etc.

Some of our recent work on entropy stable methods

- More general entropy stable "modal" DG formulations.
- Network domains, reduced order modeling
- Non-conforming meshes (Mario Bencomo, DCDR Fernandez)
- Positivity preserving entropy stable schemes for compressible Navier-Stokes (Yimin Lin, T. Warburton, I. Tomas)
- Efficient implementations (with the developers of Trixi.jl)

Chan (2018). *On discretely entropy conservative and entropy stable discontinuous Galerkin methods*.

Wu, Chan (2020). *Entropy stable discontinuous Galerkin methods for nonlinear conservation laws on networks and multi-dimensional domains*.

Chan (2020). *Entropy stable reduced order modeling of nonlinear conservation laws*.

Chan, Bencomo, Del Rey Fernandez (2021). *Mortar-based entropy-stable discontinuous Galerkin methods on non-conforming quadrilateral and hexahedral meshes*.

Chan, Lin, Warburton (2021). *Entropy stable modal discontinuous Galerkin schemes and wall boundary conditions for the compressible Navier-Stokes equation*.

Ranocha et al. (2021). Efficient implementation of modern ES and KEP DG methods. . . .

Lin, Chan, Tomas (2023). *A positivity preserving strategy for entropy stable discontinuous Galerkin discretizations of the compressible Euler and Navier-Stokes equations*.

Entropy stable nodal DG with positivity-preserving limiting

Entropy stable schemes require positivity

Entropy stable schemes require positivity of density, pressure (numerical fluxes depend on *logarithm* of density, temperature).

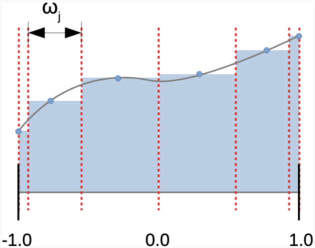

Interpretation of Lobotto nodes as a sub-cell finite volume grid.

- Hard to enforce *both* high order accuracy and positivity.
- Strategy: blend high order method with a first order positive method to retain conservation and subcell resolution.

Rueda-Ramirez, Hennemann, Hindenlang, Winters, Gassner (2021). *An entropy stable nodal DG method for the resistive MHD equations. Part II: Subcell finite volume shock capturing*.

The low order method: a global matrix formulation

Start with a naive *global* matrix formulation using forward Euler (can extend to higher order in time using SSP-RK).

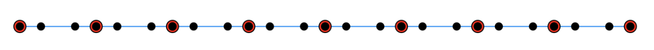

An example nodal DG discretization.

$$\mathbf{m}_i \frac{\mathbf{u}_i^{k+1} - \mathbf{u}_i}{\Delta t} + \sum_{j \in N(i)} \mathbf{Q}_{ij} \boldsymbol{f}(\mathbf{u}_j) = \mathbf{0}.$$

Equivalent to a central DG scheme.

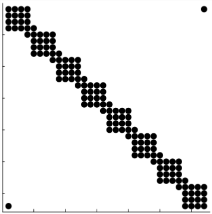

$\mathbf{Q}$ for the nodal DG example.

Can show that $\sum_j \mathbf{Q}_{ij} = 0$ and (for periodic domains) $\mathbf{Q}_{ij} = -\mathbf{Q}_{ji}$.

Enforcing positivity: a first order positive subcell scheme

Add dissipation to our global matrix formulation with forward Euler (or SSP-RK). Let $\mathbf{d}_{ij} = \mathbf{d}_{ji} > 0$ for $i \neq j$, $\sum_j \mathbf{d}_{ij} = 0$.

$$\mathbf{m}_i \frac{\mathbf{u}_i^{k+1} - \mathbf{u}_i}{\Delta t} + \sum_{j \in N(i)} \mathbf{Q}_{ij} \boldsymbol{f}(\mathbf{u}_j) - \underbrace{\mathbf{d}_{ij}\left(\mathbf{u}_j - \mathbf{u}_i\right)}_{\text{algebraic dissipation}} = \mathbf{0}. \qquad (1)$$

(Equivalent to DG with LxF interface fluxes + volume dissipation)

Use properties of $\mathbf{Q}$ to rewrite (1) in terms of "bar states"

$$\bar{\mathbf{u}}_{ij} = \frac{1}{2}\left(\mathbf{u}_i + \mathbf{u}_j\right) - \frac{\mathbf{Q}_{ij}}{\mathbf{d}_{ij}}(\mathbf{f}_j - \mathbf{f}_i), \quad \text{where } \mathbf{f}_j = \boldsymbol{f}(\mathbf{u}_j),$$

$$\frac{\mathbf{m}_i}{\Delta t}\mathbf{u}_i^{k+1} = \left(\frac{\mathbf{m}_i}{\Delta t} - \sum_{j \neq i} 2\mathbf{d}_{ij}\right)\mathbf{u}_i + \sum_{j \neq i} \frac{2\Delta t \mathbf{d}_{ij}}{\mathbf{m}_i}\bar{\mathbf{u}}_{ij}.$$

Guermond, Popov, and Tomas (2019). *Invariant domain preserving discretization-independent schemes and convex limiting for hyperbolic systems.*

Enforcing positivity: a first order positive subcell scheme

Add dissipation to our global matrix formulation with forward Euler (or SSP-RK). Let $\mathbf{d}_{ij} = \mathbf{d}_{ji} > 0$ for $i \neq j$, $\sum_j \mathbf{d}_{ij} = 0$.

$$\mathbf{m}_i \frac{\mathbf{u}_i^{k+1} - \mathbf{u}_i}{\Delta t} + \sum_{j \in N(i)} \mathbf{Q}_{ij} \boldsymbol{f}(\mathbf{u}_j) - \underbrace{\mathbf{d}_{ij}\left(\mathbf{u}_j - \mathbf{u}_i\right)}_{\text{algebraic dissipation}} = \mathbf{0}. \qquad (1)$$

(Equivalent to DG with LxF interface fluxes + volume dissipation)

Use properties of $\mathbf{Q}$ to rewrite (1) in terms of "bar states"

$$\bar{\mathbf{u}}_{ij} = \frac{1}{2}\left(\mathbf{u}_i + \mathbf{u}_j\right) - \frac{\mathbf{Q}_{ij}}{\mathbf{d}_{ij}}(\mathbf{f}_j - \mathbf{f}_i), \quad \text{where } \mathbf{f}_j = \boldsymbol{f}(\mathbf{u}_j),$$

$$\frac{\mathbf{m}_i}{\Delta t}\mathbf{u}_i^{k+1} = \left(\frac{\mathbf{m}_i}{\Delta t} - \sum_{j \neq i} 2\mathbf{d}_{ij}\right)\mathbf{u}_i + \sum_{j \neq i} \frac{2\Delta t \mathbf{d}_{ij}}{\mathbf{m}_i}\bar{\mathbf{u}}_{ij}.$$

Guermond, Popov, and Tomas (2019). *Invariant domain preserving discretization-independent schemes and convex limiting for hyperbolic systems.*

Provable positivity under a CFL condition

$$\frac{\mathbf{m}_i}{\Delta t}\mathbf{u}_i^{k+1} = \left(\frac{\mathbf{m}_i}{\Delta t} - \sum_{j\neq i} 2\mathbf{d}_{ij}\right)\mathbf{u}_i + \sum_{j\neq i}\frac{2\Delta t\mathbf{d}_{ij}}{\mathbf{m}_i}\bar{\mathbf{u}}_{ij}.$$

- Bar states $\bar{\mathbf{u}}_{ij}$ resemble a Lax-Friedrichs intermediate state, and preserve positivity if $\mathbf{d}_{ij}$ is sufficiently large

$$\bar{\mathbf{u}}_{ij} = \frac{1}{2}\left(\mathbf{u}_i + \mathbf{u}_j\right) - \frac{\mathbf{Q}_{ij}}{\mathbf{d}_{ij}}\left(\mathbf{f}_j - \mathbf{f}_i\right), \qquad \mathbf{d}_{ij} \geq \lambda_{\max}\left(\mathbf{u}_i, \mathbf{u}_j, \mathbf{Q}_{ij}\right).$$

- $\mathbf{u}_i^{k+1}$ is positive (a convex combination of $\mathbf{u}_i$ and $\bar{\mathbf{u}}_{ij}$) if

$$\Delta t \leq \min_i \frac{\mathbf{m}_i}{2\sum_{i\neq j}\mathbf{d}_{ij}}.$$

Guermond and Popov (2016). *Invariant domains and first-order continuous finite element approximation for hyperbolic systems.*

Our work: extension to compressible Navier-Stokes

- Entropy stable discretization of viscous terms $\boldsymbol{\sigma}$, which include the stress $\boldsymbol{\tau}$ + heat conduction $\boldsymbol{q}$.

$$\mathbf{M}\frac{\mathrm{d}\mathbf{u}}{\mathrm{dt}} + \sum_j \mathbf{Q}_{ij}\left(\mathbf{f}_j - \boldsymbol{\sigma}_j\right) - \mathbf{d}_{ij}\left(\mathbf{u}_j - \mathbf{u}_i\right) = \mathbf{0}.$$

- Reformulate scheme in terms of viscous bar states:

$$\bar{\mathbf{u}}_{ij} = \frac{1}{2}\left(\mathbf{u}_i + \mathbf{u}_j\right) - \frac{\mathbf{Q}_{ij}}{\mathbf{d}_{ij}}\left(\left(\mathbf{f}_j - \boldsymbol{\sigma}_j\right) - \left(\mathbf{f}_i - \boldsymbol{\sigma}_i\right)\right)$$

- Positivity of ρ, p under a (viscous) CFL condition with

$$\mathbf{d}_{ij} = \max\left(\beta(\mathbf{u}_i), \beta(\mathbf{u}_j), \lambda_{\max}(\mathbf{u}_i, \mathbf{u}_j, \mathbf{Q}_{ij}), \lambda_{\max}(\mathbf{u}_j, \mathbf{u}_i, \mathbf{Q}_{ji})\right)$$

$$\beta(\boldsymbol{u}) > |\boldsymbol{v}\cdot\boldsymbol{n}| + \frac{1}{2\rho^2 e}\left(\sqrt{\rho^2(\boldsymbol{q}\cdot\boldsymbol{n})^2 + 2\rho^2 e\left\|\boldsymbol{\tau}\cdot\boldsymbol{n} - p\boldsymbol{n}\right\|}\right) + \rho\left|\boldsymbol{q}\cdot\boldsymbol{n}\right|$$

Zhang (2017). *On positivity-preserving high order DG schemes for the compressible NS equations.*

Sparsification of low order discretization matrices

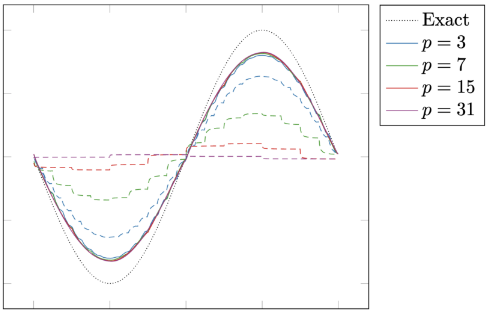

Low order advection solutions with (solid) and without (dashed) sparsification (from Pazner 2021).

- Algebraic artificial dissipation depends on discretization matrices $\Longrightarrow$ dense operators produce too much diffusion!
- Solution: use *sparse* SBP operators in the low order method.

Pazner (2021). *Sparse invariant domain preserving DG methods with subcell convex limiting.*

Sparsification of low order discretization matrices

$$\mathbf{Q} = \frac{1}{2}\begin{bmatrix} -1 & 1 & & & \\ -1 & 0 & 1 & & \\ & \ddots & \ddots & \ddots & \\ & & -1 & 0 & 1 \\ & & & -1 & 1 \end{bmatrix}$$

$$\mathbf{Q1} = \mathbf{0}, \qquad \underbrace{\mathbf{Q} + \mathbf{Q}^T = \mathbf{E}^T\mathbf{B}\mathbf{E}}_{\text{summation-by-parts property}}.$$

- Algebraic artificial dissipation depends on discretization matrices $\Longrightarrow$ dense operators produce too much diffusion!
- Solution: use *sparse* SBP operators in the low order method.

Pazner (2021). *Sparse invariant domain preserving DG methods with subcell convex limiting.*

Constructing sparse low order simplicial SBP operators

- Want to preserve conservation $\mathbf{Q}^{\text{low}}\mathbf{1} = \mathbf{0}$ and SBP property

$$\mathbf{Q}^{\text{low}} + \left(\mathbf{Q}^{\text{low}}\right)^T = \mathbf{B}.$$

- For neighboring i and j, assume

$$\left(\mathbf{Q}^{\text{low}} - \left(\mathbf{Q}^{\text{low}}\right)^T\right)_{ij} = \psi_j - \psi_i.$$

- Enforcing $\mathbf{Q}^{\text{low}}\mathbf{1} = \mathbf{0}$ equivalent to

$$\sum_j \psi_j - \psi_i = \left(-\frac{1}{2}\mathbf{B}\mathbf{1}\right)_i, \quad \text{s.t. } \boldsymbol{\psi}^T\mathbf{1} = 0.$$

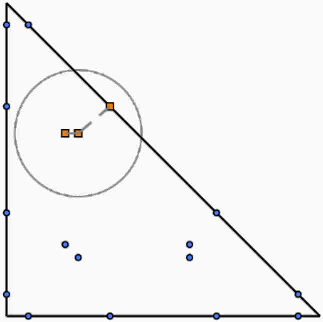

Quadrature nodes from Chen, Shu (2017) for a degree $N = 3$ SBP operator. The sparse low order operator $\mathbf{Q}^{\text{low}}$ uses the same nodes and weights.

Blending high and low order DG solutions

- Blend high and low order solutions over each element to retain accuracy where possible while ensuring positivity.

$$\mathbf{u}^{k+1} = (1-\ell)\mathbf{u}^{k+1,\text{low}} + \ell\mathbf{u}^{k+1,\text{high}}$$

- Impose minimal local bounds based on low order solution with relaxation factor α

$$\rho \geq \alpha\rho^{\text{low}}, \qquad p \geq \alpha p^{\text{low}}, \qquad \alpha \in [0,1].$$

- Local entropy inequality: preserved for element-wise blending.
- Local conservation: preserved if high and low order schemes use the same interface flux.

Convergence tests: LeBlanc and viscous shock tube

	$N=2$		$N=5$	
h	L^1 error	Rate	L^1 error	Rate
0.02	8.681×10^{-2}		5.956×10^{-2}	.
0.01	3.658×10^{-2}	1.25	1.436×10^{-2}	2.05
0.005	1.329×10^{-2}	1.46	3.630×10^{-3}	1.98
0.0025	6.015×10^{-3}	1.14	1.129×10^{-3}	1.69
0.00125	2.910×10^{-3}	1.05	5.889×10^{-4}	0.94

(a) Leblanc shock tube, relaxation factor $\alpha = 0.5$

	$N=2$		$N=3$	
h	L^1 error	Rate	L^1 error	Rate
0.025	2.305×10^{-2}		2.071×10^{-2}	
0.0125	9.858×10^{-2}	1.23	6.749×10^{-3}	1.62
0.00625	3.382×10^{-3}	1.54	1.278×10^{-3}	2.40
0.003125	5.765×10^{-4}	2.55	1.163×10^{-4}	3.45
0.0015625	8.836×10^{-5}	2.71	1.269×10^{-5}	3.20

(b) 1D viscous shock, $\mathrm{Re} = 1000$, relaxation factor $\alpha = 0.5$

Viscous shock is run at Mach 20 to generate positivity violations.

Isentropic vortex with small minimum density

	$N=2$		$N=3$		$N=4$	
h	L^2 error	Rate	L^2 error	Rate	L^2 error	Rate
2.5	1.148×10^{0}		5.958×10^{-1}	1.28	4.073×10^{-1}	
1.25	4.865×10^{-1}	1.24	1.905×10^{-1}	1.64	8.987×10^{-2}	2.18
0.625	1.223×10^{-1}	1.99	2.308×10^{-2}	3.05	1.511×10^{-2}	2.57
0.3125	1.706×10^{-2}	2.84	2.393×10^{-3}	3.27	1.915×10^{-4}	6.30

(c) Quadrilateral meshes, relaxation factor $\alpha = 0.5$

	$N=2$		$N=3$		$N=4$	
h	L^2 error	Rate	L^2 error	Rate	L^2 error	Rate
2.5	7.887×10^{-1}		5.034×10^{-1}		4.059×10^{-1}	
1.25	3.834×10^{-1}	1.04	1.881×10^{-1}	1.42	9.890×10^{-2}	2.04
0.625	8.993×10^{-2}	2.09	2.944×10^{-2}	2.68	1.578×10^{-2}	2.65
0.3125	1.298×10^{-2}	2.79	2.606×10^{-3}	3.50	4.258×10^{-4}	5.21

(d) Triangular meshes, relaxation factor $\alpha = 0.5$

Challenging vortex parameters: $\rho_{\min} = 2.145 \times 10^{-3}$

Compressible Euler: double Mach reflection

(a) Subcell positivity-preserving entropy stable nodal DG, $\alpha = 0.5, T = .2$

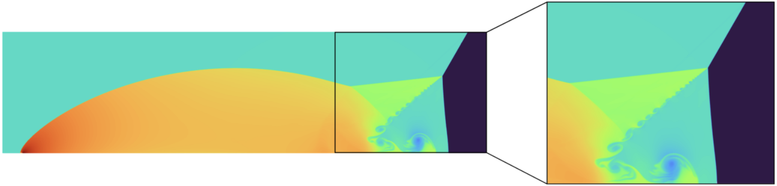

(b) Subcell invariant domain preserving nodal DG (Pazner 2021), $T = .275$

Density for $N = 3$ entropy stable DG (250×875 elements) and a reference solution (600×2400 elements). Note: positivity is sensitive to the wall boundary treatment!

---

van der Vegt and Ven (2002). *Slip flow boundary conditions in dG discretizations of the Euler*

Compressible Euler: Sedov blast wave

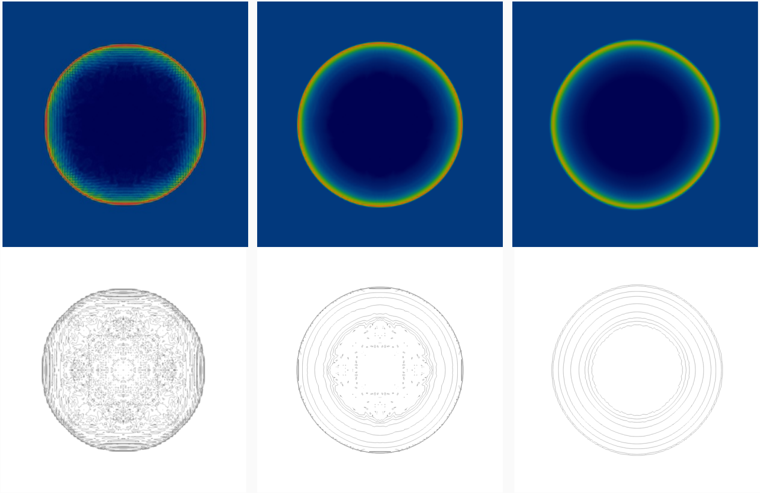

(a) $\alpha = 0.1$ **(b)** $\alpha = 0.5$ **(c)** $\alpha = 0.1$ + shock capturing

Quadrilateral meshes with 100^2 degree $N = 3$ elements.

Compressible Euler: Sedov blast wave

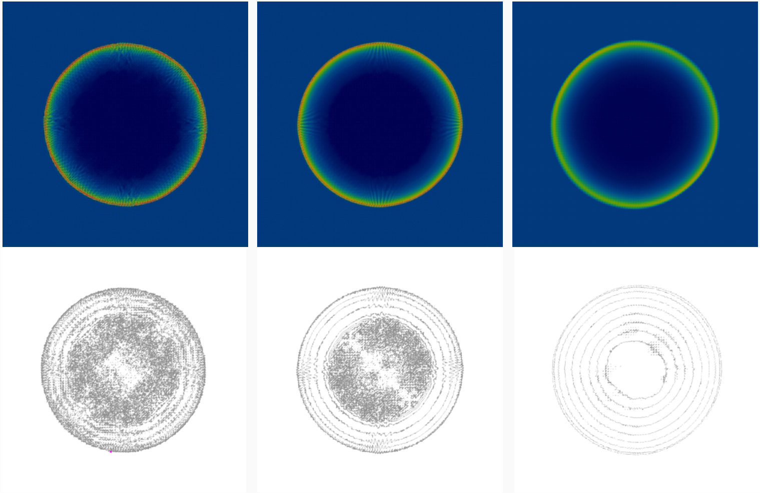

(a) $\alpha = 0.1$ **(b)** $\alpha = 0.5$ **(c)** $\alpha = 0.1$ + shock capturing

Triangular meshes with 100^2 degree $N = 3$ elements.

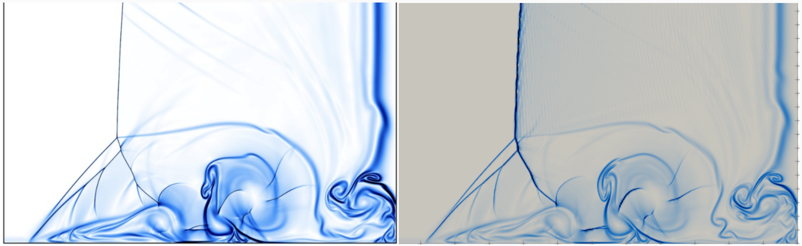

(a) Reference solution (512M nodes) **(b)** Degree $N = 3$, 600×300 grid

Comparison of a 4th order positivity-preserving entropy stable DG method with a "grid-converged" reference solution from Guermond et al. (2022).

Guermond, Kronbichler, Maier, Popov, Tomas (2022). *On the implementation of a robust and efficient finite element-based parallel solver for the compressible Navier-Stokes equations.*

Many phenomena are sensitive to “shock capturing”

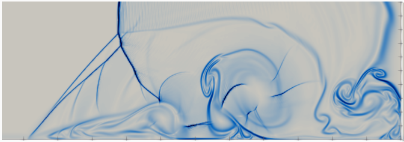

(a) Degree $N = 3$, 600×300 grid

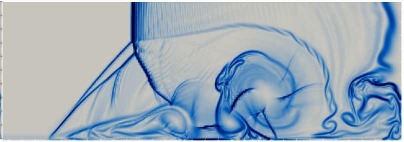

(b) Degree $N = 2$, 400×200 grid

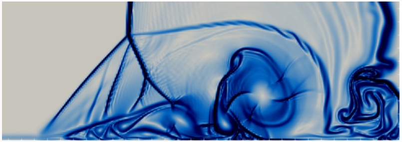

(c) With entropy stable shock capturing ($N = 2$, 400×200)

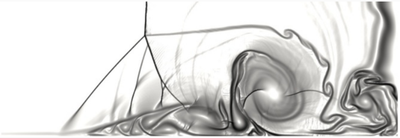

(d) Dzanic and Witherden ($N = 4$, 800×400 grid)

Hennemann et al. (2021). *A provably entropy stable subcell shock capturing approach for high order split form DG methods for the compressible Euler equations.*

Dzanic, Witherden (2022). *Positivity-preserving entropy-based adaptive filtering for discontinuous spectral element methods.*

Sensitivity to shock capturing at higher Reynolds numbers

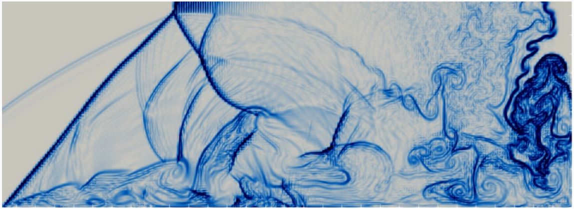

Degree $N = 2$, 200×100 mesh with positivity parameter $\alpha = 0.1$.

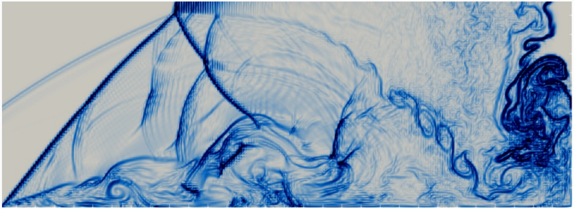

Same setup with positivity parameter $\alpha = 0.5$.

Hennemann et al. (2021). "A provably ES subcell shock capturing approach for high order split form DG for the compressible Euler equations".

Sensitivity to shock capturing at higher Reynolds numbers

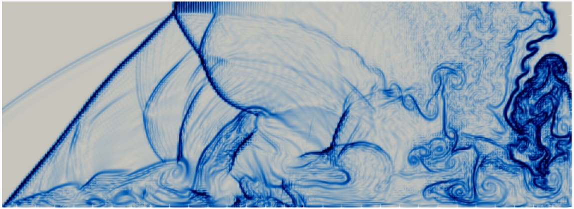

Degree $N = 2$, 200×100 mesh with positivity parameter $\alpha = 0.1$.

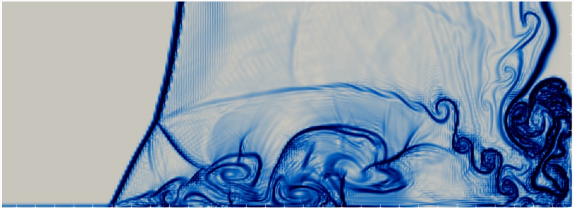

Positivity parameter $\alpha = 0.1$ with Hennemann (2021) shock capturing.

Hennemann et al. (2021). "A provably ES subcell shock capturing approach for high order split form DG for the compressible Euler equations".

From subcell limiting to a cell entropy inequality

Subcell *resolution* vs subcell *blending*

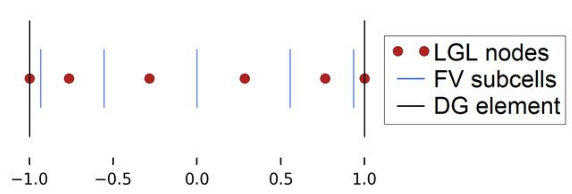

Figure from Hennemann et al. 2021.

- The low order method has subcell *resolution*, but element-wise constant high/low order blending.
- It is possible to perform blending at a *subcell* level; however, subcell blending does not necessarily preserve entropy stability!
- Not all entropy inequalities preserve high order accuracy . . .

Hennemann et al. (2021). "A provably ES subcell shock capturing approach for high order split form DG for the compressible Euler equations".

Start with a (possibly non-ES) semi-discrete nodal DG formulation:

$$\mathbf{m}_i \frac{\mathrm{d}\mathbf{u}_i}{\mathrm{dt}} + \mathbf{r}_i + \left(\delta_{i,N+1}\mathbf{f}_R^* - \delta_{i,1}\mathbf{f}_L^*\right) = \mathbf{0}, \qquad \underbrace{\sum \mathbf{r}_j = 0}_{\text{conservation}}$$

This is algebraically equivalent to the following scheme

$$\mathbf{m}_i \frac{\mathrm{d}\mathbf{u}_i}{\mathrm{dt}} + \bar{\mathbf{f}}_{i+1} - \bar{\mathbf{f}}_i = \mathbf{0},$$

where $\bar{\mathbf{f}}_i$ are "reconstructed" finite volume-type fluxes

$$\begin{aligned} \bar{\mathbf{f}}_1 &= \mathbf{f}_L^* \\ \bar{\mathbf{f}}_{1+i} &= \sum_{j=1}^{i} \mathbf{r}_j, \quad i = 1, \ldots, N+1 \\ \bar{\mathbf{f}}_{N+2} &= \mathbf{f}_R^*. \end{aligned}$$

Subcell finite volume formulation

Blend high and low order schemes with subcell fluxes.

$$\mathbf{m}_i \frac{\mathrm{d}\mathbf{u}_i}{\mathrm{dt}} + \underbrace{\left[l_{i+1}\bar{\mathbf{f}}^{\mathrm{H}}_{i+1} + (1 - l_{i+1})\,\bar{\mathbf{f}}^{\mathrm{L}}_{i+1}\right]}_{\bar{\mathbf{f}}_{i+1}} - \underbrace{\left[l_i\bar{\mathbf{f}}^{\mathrm{H}}_{i} + (1 - l_{i})\,\bar{\mathbf{f}}^{\mathrm{L}}_{i}\right]}_{\bar{\mathbf{f}}_{i}} = \mathbf{0},$$

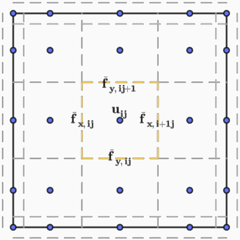

- $l_i = 1 \implies$ recovers high order nodal DG.
  $l_i = 0 \implies$ recovers low order invariant domain scheme.
- Pick largest l_i to satisfy positivity constraints while retaining as much of the high order method as possible.

Rueda-Ramírez, Andrés et al., "Subcell limiting strategies for DG spectral element methods."

Enforcing entropy stability as a pointwise constraint

- Option 1: minimum entropy principle (fully discrete).

$$s_i \geq \min_{j \in \mathcal{N}(i)} s_j^n.$$

- Option 2: semi-discrete condition on subcell fluxes

$$\left(\mathbf{v}_i - \mathbf{v}_{i-1}\right)^T \bar{\mathbf{f}}_i \leq \psi\left(\mathbf{u}_i\right) - \psi\left(\mathbf{u}_{i-1}\right)$$

	$N=2$		$N=3$		$N=4$	
K	L^2 error	Rate	L^2 error	Rate	L^2 error	Rate
5	7.498×10^{-1}		4.499×10^{-1}		3.135×10^{-1}	
10	3.343×10^{-1}	1.17	2.109×10^{-1}	1.09	1.486×10^{-1}	1.08
20	1.894×10^{-1}	0.82	1.092×10^{-1}	0.95	7.509×10^{-2}	0.98
40	9.718×10^{-2}	0.96	5.956×10^{-2}	0.87	4.160×10^{-2}	0.85
80	5.116×10^{-2}	0.93	3.186×10^{-2}	0.90	2.157×10^{-2}	0.95

Neither "pointwise" approach retains high order accuracy.

Tadmor, Eitan. "A minimum entropy principle in the gas dynamics equations."

Kuzmin, Dmitri et al., "Limiter-based entropy stabilization of semi-discrete and fully discrete schemes for nonlinear hyperbolic problems."

Enforcing a cell entropy inequality

Choose $l_1, \ldots, l_{N+2}$ over each element to enforce

$$\mathbf{v}^T \mathbf{M} \frac{\mathrm{d}\mathbf{u}}{\mathrm{dt}} \leq \left(\psi(\mathbf{u}_{N+1}) - \mathbf{v}_{N+1}^T \mathbf{f}_R^*\right) - \left(\psi(\mathbf{u}_1) - \mathbf{v}_1^T \mathbf{f}_L^*\right)$$

$$\implies \sum_{i=1}^{N+1} \mathbf{v}_i^T \left(\bar{\mathbf{f}}_{i+1}(l_{i+1}) - \bar{\mathbf{f}}_i(l_i)\right) \leq \psi(\mathbf{u}_{N+1}) - \psi(\mathbf{u}_1),$$

where $\bar{\mathbf{f}}_i(l_i) = l_i \bar{\mathbf{f}}_i^H + (1 - l_i)\bar{\mathbf{f}}_i^L$.

	$N=2$		$N=3$		$N=4$	
K	L^2 error	Rate	L^2 error	Rate	L^2 error	Rate
5	6.935×10^{-1}		2.498×10^{-1}		1.587×10^{-1}	
10	1.785×10^{-1}	1.96	7.083×10^{-2}	1.82	2.000×10^{-2}	2.99
20	4.126×10^{-2}	1.11	8.898×10^{-3}	2.99	9.557×10^{-4}	4.39
40	6.714×10^{-3}	2.62	8.163×10^{-4}	3.45	3.142×10^{-5}	4.93
80	1.210×10^{-3}	2.74	4.208×10^{-5}	4.28	1.530×10^{-6}	4.36

Enforcing a cell entropy inequality recovers high order accuracy.

Formulation as an optimization problem

Maximizing limiting factors l_i while enforcing cell entropy inequality

$$\sum_{i=1}^{N+1} \mathbf{v}_i^T \left(\bar{\mathbf{f}}_{i+1}(l_{i+1}) - \bar{\mathbf{f}}_i(l_i)\right) \leq \psi(\mathbf{u}_{N+1}) - \psi(\mathbf{u}_1)$$

can be posed as a continuous knapsack problem, which admits a fast and explicit $O(n\log(n))$ solution algorithm.

$$\begin{aligned} \max_{l_i} \quad & \sum_{i=1}^{N} l_i \\ \text{s.t.} \quad & \sum_{i=1}^{N} a_i l_i \leq b \\ & 0 \leq l_i \leq l_i^{\mathrm{C}} \end{aligned}$$

where $l_i^{\mathrm{C}} \leq 1$ is a limiting factor upper bound to ensure positivity.

Modified Sod shock tube

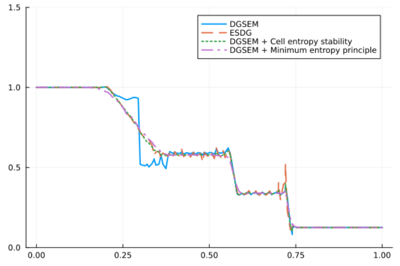

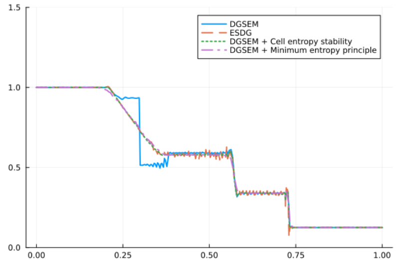

Naive (DGSEM) and entropy stable (ESDG) DG discretizations with different limiting strategies for enforcing an entropy principle.

An entropy glitch appears without some form of entropy inequality (e.g., minimum entropy principle or cell entropy inequality).

2D KPP problem

(a) Shock capturing only

(b) Shock capturing and cell entropy inequality

Hennemann (2021) shock capturing with and without cell entropy inequality (degree $N = 3, 128 \times 128$ elements).

Hennemann et al. (2021). *A provably entropy stable subcell shock capturing approach for high order split form DG methods for the compressible Euler equations.*

Kelvin Helmholtz instability

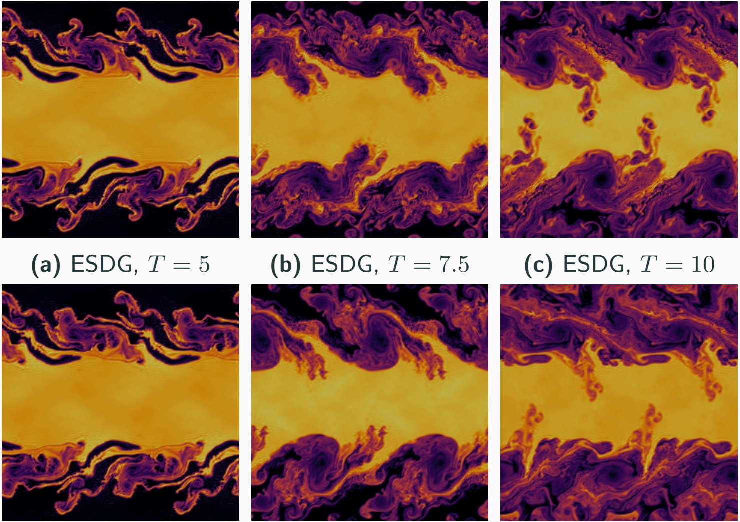

(a) ESDG, $T = 5$ **(b)** ESDG, $T = 7.5$ **(c)** ESDG, $T = 10$

(d) DGSEM, $T = 5$ **(e)** DGSEM, $T = 7.5$ **(f)** DGSEM, $T = 10$

Long-time KHI simulation with positivity and cell entropy inequality enforced.

Compressible Euler - Mach 2000 Astrophysical jet

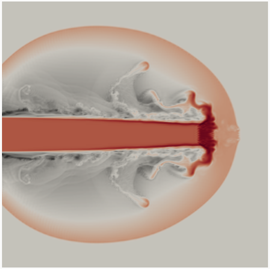

(a) Subcell limited DGSEM + cell entropy inequality

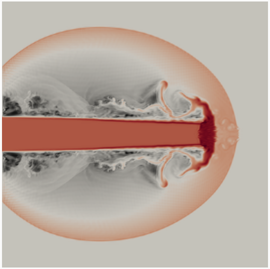

(b) Subcell limited ESDG + cell entropy inequality

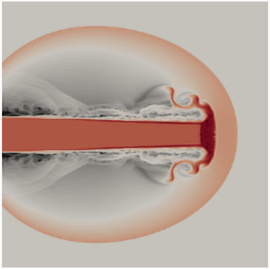

(c) ESDG with element-wise positivity limiting

Density for degree $N = 3,\ 150 \times 150$ elements. We enforce the relaxed positivity bounds $\rho > 0.5\rho^{\mathrm{L}},\ \rho e > 0.5\,(\rho e)^{\mathrm{L}}$.

Conclusions and acknowledgements

- Positivity preserving limiters enable robust entropy stable nodal DG simulations of compressible flow.
- We can enforce a (high order?) cell entropy inequality for standard nodal DG using subcell limiting.

This work is supported by DMS-1943186 and DMS-2231482.

Thank you! Questions?

Lin, Chan (2023). *High order entropy stable discontinuous Galerkin spectral element methods through subcell limiting*.

Lin, Chan, Tomas (2022). *A positivity preserving strategy for entropy stable discontinuous Galerkin discretizations of the compressible Euler and Navier-Stokes equations*.

Additional slides

Subcell limiting for compressible Navier-Stokes

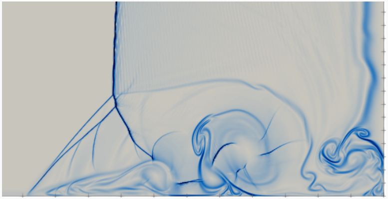

(a) $N = 3$, 600×300 grid.
ESDG + element-wise limiting.

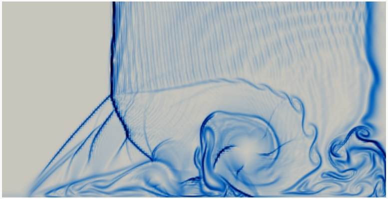

(b) $N = 3$, 300×150 grid.
ESDG + element-wise limiting.

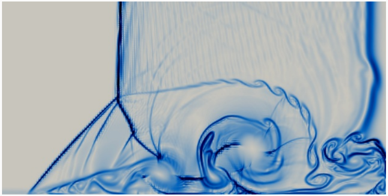

(c) $N = 3$, 300×150 grid.
DGSEM + subcell limiting

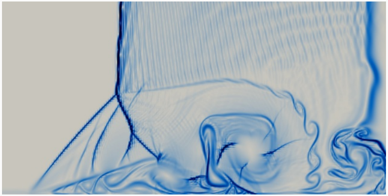

(d) $N = 3$, 300×150 grid.
ESDG + subcell limiting

Daru-Tenaud simulations with positivity and cell entropy inequality.